

High frequency permeability of the composite with ferromagnetic spherical shells

A.O. Sboychakov¹

¹*Institute for Theoretical and Applied Electrodynamics,
Russian Academy of Sciences, 125412 Moscow, Russia*

(Dated: June 13, 2025)

The paper studies high-frequency permeability of the composite materials consisting of hollow ferromagnetic particles embedded into the non-magnetic media. We model the ferromagnetic particles in composite by spherical shell: the thickness of the ferromagnetic region d compared to the particles' diameter D can vary in a wide range, from $d \ll D$ to $d \sim D$. We assume that the magnetization distribution in such a particle is non-uniform, but forms a vortex-like structure: the magnetization is twisted in some plain outside two vortex cores placed at the poles of the particle. The high-frequency permeability of such a composite material has been studied in the limit of non-interacting particles. We study the dependence of the permeability on the ratio d/D . It was shown, in particular, that in the limit $d/D \ll 1$ the frequency dependence of the particle's susceptibility is quite similar to that for the thin film. At the same time, the magnetization oscillations in the ac field are non-homogeneous.

PACS numbers: 75.78.-n, 75.75.Jn, 75.75.-c

I. INTRODUCTION

Magnetic composites are interesting both from a fundamental point of view and for a large number of technical applications, for many of which it is important to know the system's response to an external alternating magnetic field. The internal structure of composite materials is extremely diverse. In this paper, we will be interested in materials consisting of non-contacting ferromagnetic particles with spherical or near spherical shape, separated by a non-magnetic dielectric matrix. Due to the peculiarities of the manufacturing technology, it often turns out that ferromagnetic particles contain a hollow region in their centers¹⁻⁶. The characteristic sizes of such particles D can vary in a wide range. For example, in Ref. 1, the particles in the composites synthesized had sizes of about 500 nm with a characteristic thickness of the ferromagnetic region $d \sim 80$ nm. Similar^{4,6}, or slightly larger ($D \sim 1 \mu\text{m}$ ⁵) particle sizes were obtained in materials studied in Refs. 4-6. Composites with particles of larger² ($D \sim 30-100 \mu\text{m}$) and smaller³ ($D \sim 100$ nm) sizes have been also synthesized. The ratio of the thickness of the ferromagnetic layer d to the particle's size D can also vary in a wide range. Thus, according to the Table 2 of Ref. 3, the ratio of d/D for different samples varied from about 0.1 to about 0.3. As for the larger particles, studied in the Ref. 2, the d/D ratio could be about 0.05.

In this paper, we focus on the particle sizes $D \sim 0.5-1 \mu\text{m}$, characteristic of composites synthesized, in particular, in Refs. 4-6. Such particle sizes are not too large, which points in favor of their homogeneous structure. At the same time, for such particle sizes the condition $l_{ex}/D \ll 1$ is satisfied with good accuracy, where l_{ex} is the exchange length of the ferromagnet, which is of the order of several nanometers⁷. We model the ferromagnetic particles in composite by spherical shells with outer radius R_2 , and the inner radius R_1 , while $d = R_2 - R_1$

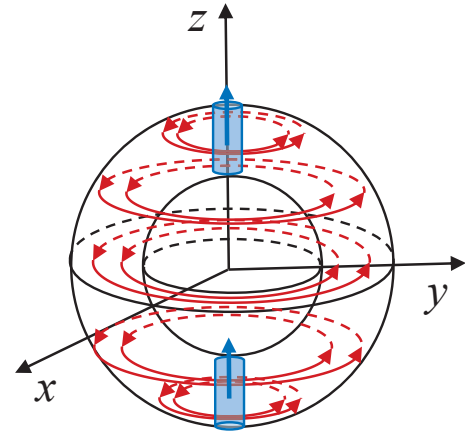


FIG. 1. The vortex magnetic configuration of the spherical shell. Outside the vortex cores, located at poles of the particle, the magnetization vectors lie in the xy plane and form a system of circles, as shown schematically in the figure.

is the thickness of the ferromagnetic region. For further consideration, it will be convenient for us to introduce the quantity $R_0 = (R_2 + R_1)/2$ – the radius of the central layer. Thus, for the particle sizes under consideration, we have $l_{ex}/R_0 \sim 10^{-2} \ll 1$.

In this paper we assume that the distribution of the magnetization in a particle is non-homogeneous, but forms a vortex-like structure: with the exception of the area near the poles, the magnetization vectors lie in the same plane (xy plane) and are directed parallel to the surface of the particle. Near the poles, there are two domains with magnetization vectors directed parallel to the z axis of the particle. The typical domain sizes are $r_0 \times r_0 \times d$, where $r_0 \sim l_{ex}$. Schematically, this structure is shown in the Fig. 1. Such a configuration was studied, e.g., in Refs. 8-11. In Ref 11 it has been shown experimentally using the electron holography technique, that the

static magnetic configuration of the hollow ferromagnetic particle has indeed the vortex-like structure. Frequency dependence of the permeability for vortex magnetic configuration has been studied theoretically in Ref. 8. However, the particle sizes, studied their ($R_0 \sim 100$ nm), are about order of magnitude smaller than that studied in this paper. In our case, as we will show below, the main contribution, determining the frequency dependence of the permeability, is coming from the magnetostatic energy, but not from the exchange energy.

Since the magnetization in a particle is spatially inhomogeneous, the oscillations of the magnetization vectors under the action of an alternating magnetic field will also be inhomogeneous. We take this fact into account when determining the susceptibility of both the particle and the composite as a whole. The plan of this work is as follows. In Section II, we will derive the linearized Landau-Lifshitz equations for the magnetic configuration described above. In section III, the formula for the magnetic permeability of the composite will be obtained. The results of the numerical calculation of the magnetic permeability, as well as the properties of the magnetization oscillations in the field at the frequency corresponding to the main resonance will be analyzed. In section IV, an analytical formula for the magnetic permeability of the composite in the limit of $d/R_0 \rightarrow 0$ and $l_{ex}/R_0 \rightarrow 0$ will be derived. In section V, the particle's self-oscillations are considered. The stability analysis of the considered configuration is performed. Section VI is devoted to the discussion of the results obtained. Some details of the calculations are provided in the Appendix.

II. LANDAU-LIFSHITZ EQUATION FOR THE FERROMAGNETIC SPHERICAL SHELL

We start with the Landau-Lifshitz equations, which have the form⁷

$$\frac{\partial \mathbf{M}}{\partial t} = \gamma \mathbf{M} \times \frac{\delta U}{\delta \mathbf{M}} + \frac{\alpha}{M_s} \mathbf{M} \times \frac{\partial \mathbf{M}}{\partial t} - \gamma \mathbf{M} \times \mathbf{h}, \quad (1)$$

where \mathbf{M} is the magnetization of the particle, M_s is the saturation magnetization, γ is the gyromagnetic ratio, α is the decay parameter, U is the total magnetic energy of the particle, and \mathbf{h} is the external alternating magnetic field. The magnetic energy of the particle U includes three terms, $U = U_m + U_a + U_{ex}$, where U_m is the magnetostatic energy, U_a is the energy of magnetic anisotropy, and U_{ex} is the energy of the exchange interaction. Let us first consider the energy of magnetic anisotropy. We will assume that the particle has uniaxial magnetic anisotropy, so we can write⁷ [here and further, the summation over the double indices (e.g., $\alpha = x, y, z$) is implied]

$$U_a = -\frac{\beta}{2} \int_V d^3 \mathbf{r} M^\alpha N_{\alpha\beta} M^\beta, \quad (2)$$

where $\beta = H_a/M_s$ (H_a is the anisotropy field), and $N_{\alpha\beta}$ is the magnetic anisotropy tensor, which, in general, depends on the coordinates. In this paper, we will assume that at each point the anisotropy axis lies in the xy plane and is directed parallel to the tangent to the particle's boundary, i.e. in the equilibrium configuration shown in Fig. 1, the direction of the magnetization (everywhere except the vortex core) and the anisotropy axis coincide. For this configuration, the anisotropy tensor can be written in the matrix form as

$$\hat{N}(\mathbf{r}) = \begin{pmatrix} \sin^2 \varphi & -\sin \varphi \cos \varphi & 0 \\ -\sin \varphi \cos \varphi & \cos^2 \varphi & 0 \\ 0 & 0 & 0 \end{pmatrix}, \quad (3)$$

where φ is the azimuthal angle of the spherical coordinate system. The magnetostatic energy has the form⁷

$$U_m = -\frac{1}{2} \int_V d^3 \mathbf{r} \mathbf{M} \mathbf{H}^{\text{in}}[\mathbf{M}], \quad \mathbf{H}^{\text{in}}[\mathbf{M}] = -\frac{\partial \Psi[\mathbf{M}]}{\partial \mathbf{r}}, \quad (4)$$

where $\Psi[\mathbf{M}]$ is the potential of the magnetic field created by the magnetic moments of the particle. It is equal to

$$\begin{aligned} \Psi[\mathbf{M}] &= -\int_V d^3 \mathbf{r}' \frac{\text{div}' \mathbf{M}(\mathbf{r}')}{|\mathbf{r} - \mathbf{r}'|} + \int_S dS' \frac{\mathbf{M}(\mathbf{r}')}{|\mathbf{r} - \mathbf{r}'|} \\ &= \int_V d^3 \mathbf{r}' \mathbf{M}(\mathbf{r}') \frac{\partial}{\partial \mathbf{r}'} \frac{1}{|\mathbf{r} - \mathbf{r}'|}. \end{aligned} \quad (5)$$

Finally, the exchange energy is⁷

$$U_{ex} = \frac{l_{ex}^2}{2} \int_V d^3 \mathbf{r} \frac{\partial M^\alpha}{\partial x^\beta} \frac{\partial M_\alpha}{\partial x_\beta}. \quad (6)$$

In all formulas above, the three-dimensional integrals are taken over the volume of the ferromagnetic region of the particle V , and the surface integral is taken over its inner and outer surfaces.

Since the particle has a spherical shape, it will be convenient for us to switch from the Cartesian coordinate system $x^\alpha = \{x, y, z\}$ to the spherical one $x^a = \{r, \theta, \varphi\}$. In addition, we will also work with vectors in a spherical coordinate system. The latter are related to vectors in the Cartesian coordinate system by the expressions¹²

$$A^\alpha = \frac{\partial x^\alpha}{\partial x^a} A^a, \quad A^a = \frac{\partial x^a}{\partial x^\alpha} A^\alpha. \quad (7)$$

We also introduce the metric tensor

$$g_{ab} = \text{diag}(1, r^2, r^2 \sin^2 \theta). \quad (8)$$

In a spherical coordinate system, the anisotropy tensor takes the form

$$N_{ab} = r^2 \sin^2 \theta \begin{pmatrix} 0 & 0 & 0 \\ 0 & 0 & 0 \\ 0 & 0 & 1 \end{pmatrix}, \quad (9)$$

and the energy of the anisotropy is equal to

$$U_a = -\frac{\beta}{2} \int_{R_1}^{R_2} r^4 dr \int d\Omega \sin^2 \theta (M^\varphi)^2, \quad (10)$$

where $d\Omega = \sin \theta d\theta d\varphi$. The potential of the magnetic field can be rewritten as

$$\Psi[\mathbf{M}] = \int_{R_1}^{R_2} r'^2 dr' \int d\Omega' M^a(\mathbf{r}') \frac{\partial}{\partial x'^a} \frac{1}{|\mathbf{r} - \mathbf{r}'|}. \quad (11)$$

The exchange energy will take the form

$$U_{ex} = \frac{l_{ex}^2}{2} \int_{R_1}^{R_2} r^2 dr \int d\Omega M_{;b}^a M_a^{;b} = \frac{l_{ex}^2}{2} \int d\Omega \left[r^2 M^a M_a^{;r} \right]_{r=R_1}^{r=R_2} - \frac{l_{ex}^2}{2} \int_{R_1}^{R_2} r^2 dr \int d\Omega M^a M_a^{;b}, \quad (12)$$

where, in the latter equation, we clearly distinguished the surface and the volume contributions to the exchange energy. In Eq. (12), the symbol ‘;’ stands for the covariant derivative¹². Finally, in the spherical coordinate system, the Landau-Lifshitz equations have the form

$$\frac{\partial M^a}{\partial t} = \sqrt{g} g^{ab} \epsilon_{bcd} M^c \left[\gamma g^{de} \frac{\delta U}{\delta M^e} + \frac{\alpha}{M_s} \frac{\partial M^d}{\partial t} - h^d \right], \quad (13)$$

where $\sqrt{g} = r^2 \sin \theta$ and ϵ_{bcd} is the Levi-Civita symbol ($\epsilon_{r\theta\varphi} = 1$).

Our aim is to find a linear response of the system to an alternating magnetic field. To do this, we linearize Eq (13) by representing the magnetization as $M^a = M_0^a + m^a(t)$, where M_0^a is the equilibrium magnetization of the particle. Following Ref. 10, we will assume that outside the vortex core, the equilibrium magnetization of the particle is

$$M_0^\alpha = M_s \begin{pmatrix} -\sin \varphi \\ \cos \varphi \\ 0 \end{pmatrix}, \quad M_0^a = \frac{M_s}{r \sin \theta} \begin{pmatrix} 0 \\ 0 \\ 1 \end{pmatrix}, \quad (14)$$

that is, only the φ component of M_0^a is nonzero. Next, in Ref. 10 it was also shown that the longitudinal dimensions of the r_0 domains located at the poles of the particle are small ($r_0 \sim l_{ex} \ll R_0$). Therefore, we will neglect the

presence of these domains wherever it is possible. Thus, it is easy to see that, ignoring the vortex core, we have $\Psi[\mathbf{M}_0] = 0$. The energy of magnetic anisotropy in equilibrium is $U_a = -\beta M_s^2 V/2$. As for the exchange energy, it logarithmically diverges at the poles of the particle, i.e. for $\theta \rightarrow 0$ or π , if we extend the expression (14) to the entire definition area. Therefore, when calculating the exchange energy, we will integrate the diverging term over θ within the range $l_{ex}/R_0 < \theta < \pi - l_{ex}/R_0$, assuming that the contribution to U_{ex} from vortex core is small. Taking all aforementioned into account, it can be shown that the following equality is satisfied with a good accuracy:

$$\epsilon_{abc} M^b g^{cd} \frac{\delta U[\mathbf{M}]}{\delta M^d} \Big|_{\mathbf{M}=\mathbf{M}_0} = 0, \quad (15)$$

that is, configuration (14) does correspond to some extremum of energy. In Section V, we will show that this extremum is a minimum (generally speaking, it is not necessarily global). In addition to Eq. (15), the boundary conditions to the Landau-Lifshitz equations, following from the expression for the surface term in the exchange energy⁷, are satisfied:

$$\epsilon_{abc} M^b M^{c;r} \Big|_{r=R_{1,2}}^{\mathbf{M}=\mathbf{M}_0} = 0. \quad (16)$$

Expanding Eq. (13) around M_0^a to the first order in $m^a(t)$, we can obtain linearized Landau-Lifshitz equations. However, it will be more convenient for us to work not with the vector m^a , whose components have different dimensions, but with an object defined as (no summation on a)

$$\tilde{m}^a = \begin{pmatrix} m^r \\ r m^\theta \\ r m^\varphi \end{pmatrix}, \quad \tilde{m}^a = \chi^a m^a, \quad \chi^a = \begin{pmatrix} 1 \\ r \\ r \end{pmatrix}, \quad \tilde{m}_a = \frac{1}{\chi^a} m_a. \quad (17)$$

Objects of the type \tilde{m}^a are not vectors (let’s call them “pseudo-vectors”) in the sense that they are not transformed according to Eq. (7), but all components of \tilde{m}^a have the same dimension, coinciding with that in the Cartesian coordinate system. Similarly, covariant and contrvariant “pseudotensors” of the second rank can be introduced. Substituting the formulas (4), (10)–(12), (14), and (17) into Eq. (13) and linearizing it by \tilde{m}^a , we obtain the following equations

$$\begin{aligned} -\frac{1}{\omega_s} \frac{\partial \tilde{m}^\theta}{\partial t} + \frac{\alpha}{\omega_s} \frac{\partial \tilde{m}^r}{\partial t} + \beta \tilde{m}^r - \frac{\partial \Psi[\tilde{\mathbf{m}}]}{\partial r} - l_{ex}^2 \left[\Delta \tilde{m}^r + \left(\frac{1}{\sin^2 \theta} - 2 \right) \frac{\tilde{m}^r}{r^2} - \frac{2}{r^2} \left(\frac{\partial \tilde{m}^\theta}{\partial \theta} + \cot \theta \tilde{m}^\theta \right) \right] &= \tilde{h}^r, \\ \frac{1}{\omega_s} \frac{\partial \tilde{m}^r}{\partial t} + \frac{\alpha}{\omega_s} \frac{\partial \tilde{m}^\theta}{\partial t} + \beta \tilde{m}^\theta + \frac{1}{r} \frac{\partial \Psi[\tilde{\mathbf{m}}]}{\partial \theta} - l_{ex}^2 \left[\Delta \tilde{m}^\theta + \frac{2}{r^2} \frac{\partial \tilde{m}^r}{\partial \theta} \right] &= \tilde{h}^\theta, \end{aligned} \quad (18)$$

where Δ is the Laplace operator, $\omega_s = \gamma M_s$, and

$$\Psi[\tilde{\mathbf{m}}] = \int_{R_1}^{R_2} r'^2 dr' \int d\Omega' \left[\tilde{m}^r(\mathbf{r}') \frac{\partial}{\partial r'} + \frac{\tilde{m}^\theta(\mathbf{r}')}{r'} \frac{\partial}{\partial \theta'} \right] \frac{1}{|\mathbf{r} - \mathbf{r}'|}. \quad (19)$$

Note that for the considered equilibrium magnetic configuration (14), the φ component of magnetization dropped out from the equations (18), we always have $\tilde{m}^\varphi = 0$. The boundary conditions to this system of equations are obtained from Eq. (16) by substitution $M^a = M_0^a + \tilde{m}^a/\kappa^a$ and linearization by \tilde{m}^a . Since for the equilibrium configuration under consideration $M_0^{a;r} = 0$, the boundary conditions are reduced to (c.f. with Refs. 13 and 14)

$$\left. \frac{\partial \tilde{m}^r}{\partial r} \right|_{r=R_{1,2}} = 0, \quad \left. \frac{\partial \tilde{m}^\theta}{\partial r} \right|_{r=R_{1,2}} = 0. \quad (20)$$

Thus, we derived the system of two linear integro-differential equations for the components \tilde{m}^r and \tilde{m}^θ . We will solve this system by expanding the magnetiza-

tion components into a series of orthogonal functions

$$\tilde{m}^a(\mathbf{r}) = \sum_{k=0}^{\infty} \sum_{l=0}^{\infty} \sum_{m=-l}^l \tilde{m}^{aklm} f_k(r) Y_l^m(\theta, \varphi), \quad (21)$$

where $Y_l^m(\theta, \varphi)$ are spherical harmonics. As for the radial functions, they should be orthogonal with weight r^2 , i.e.,

$$\frac{1}{V} \int_{R_1}^{R_2} r^2 dr f_k(r) f_{k'}(r) = \delta_{kk'}. \quad (22)$$

They also should satisfy the boundary conditions

$$\left. \frac{\partial f_k(r)}{\partial r} \right|_{r=R_{1,2}} = 0, \quad (23)$$

following from the conditions (20). The algorithm of the construction of such functions is described in the Appendix. The transformation, inverse to Eq. (21), is

$$\tilde{m}^{aklm} = \frac{1}{V} \int_V d^3\mathbf{r} \tilde{m}^a(\mathbf{r}) f_k(r) Y_l^m(\theta, \varphi)^*. \quad (24)$$

Substituting Eq. (21) into Eq. (18), multiplying both parts by $f_k(r) Y_l^m(\theta, \varphi)^*$ and integrating over the volume of the particle, after simple but cumbersome calculations, we obtain

$$\begin{aligned} & -\frac{1}{\omega_s} \frac{\partial \tilde{m}^{\theta klm}}{\partial t} + \frac{\alpha}{\omega_s} \frac{\partial \tilde{m}^{rklm}}{\partial t} + \beta \tilde{m}^{rklm} + \sum_{k'=0}^{\infty} \left[\frac{4\pi F_{kk'l}^{rr}}{2l+1} + a_{ex}^2 (G_{kk'}^r + (l^2 + l + 2)G_{kk'}^0) \right] \tilde{m}^{rk'l'm} \\ & - (a_{ex}^{(m)})^2 \sum_{k'=0}^{\infty} \sum_{l'=|m|}^{\infty} L_{ll'}^{(m)}(a_{ex}) G_{kk'}^0 \tilde{m}^{rk'l'm} + \sum_{k'=0}^{\infty} \sum_{l'=|m|}^{\infty} \left[\frac{4\pi F_{kk'l}^{r\theta}}{2l+1} - a_{ex}^2 G_{kk'}^0 \right] D_{ll'}^{(m)} \tilde{m}^{\theta k'l'm} = \tilde{h}^{rklm}, \\ & \frac{1}{\omega_s} \frac{\partial \tilde{m}^{rklm}}{\partial t} + \frac{\alpha}{\omega_s} \frac{\partial \tilde{m}^{\theta klm}}{\partial t} + \beta \tilde{m}^{\theta klm} + \sum_{k'=0}^{\infty} \sum_{l'=|m|}^{\infty} \left[\sum_{n=|m|}^{\infty} \frac{4\pi F_{kk'n}^{\theta\theta}}{2n+1} D_{nl}^{(m)*} D_{nl'}^{(m)} + \right. \\ & \left. + a_{ex}^2 \delta_{ll'} (G_{kk'}^r + l(l+1)G_{kk'}^0) \right] \tilde{m}^{\theta k'l'm} + \sum_{k'=0}^{\infty} \sum_{l'=|m|}^{\infty} \left[\frac{4\pi F_{kk'l}^{\theta r}}{2l'+1} - a_{ex}^2 G_{k'k}^0 \right] D_{l'l}^{(m)*} \tilde{m}^{rk'l'm} = \tilde{h}^{\theta klm}, \quad (25) \end{aligned}$$

where $a_{ex} = l_{ex}/R_0$, $[a_{ex}^{(0)}]^2 = a_{ex}^2 \ln(1/a_{ex})$, $a_{ex}^{(m)} = a_{ex}$ if $m \neq 0$, \tilde{h}^{aklm} are the components of the magnetic field decomposition defined similarly to Eq. (24), and the remaining parameters not defined above are given below. Namely, we introduce the following notation:

$$D_{ll'}^{(m)} = \int d\Omega \frac{\partial Y_l^{m*}(\theta, \varphi)}{\partial \theta} Y_{l'}^m(\theta, \varphi), \quad (26)$$

$$L_{ll'}^{(0)}(a_{ex}) = \sqrt{2l+1} \sqrt{2l'+1} |P_l^0(a_{ex}) P_{l'}^0(a_{ex})|, \quad (27)$$

$$L_{ll'}^{(m)}(a_{ex}) = \sqrt{\frac{(2l+1)(l-m)!}{(l+m)!}} \sqrt{\frac{(2l'+1)(l'-m)!}{(l'+m)!}} \times \int_0^{1-a_{ex}} dx \frac{P_l^m(x) P_{l'}^m(x)}{1-x^2}, \quad m \neq 0, \quad (28)$$

where $P_l^m(x)$ are the associated Legendre polynomials,

$$G_{kk'}^0 = \frac{R_0^2}{V} \int_{R_1}^{R_2} dr f_k(r) f_{k'}(r), \quad (29)$$

$$C_{kk'}^r = \frac{R_0^2}{V} \left\{ \int_{R_1}^{R_2} dr \frac{\partial}{\partial r} [r f_k(r)] \frac{\partial}{\partial r} [r f_{k'}(r)] - \right. \quad (30)$$

$$\left. - [R_2 f_k(R_2) f_{k'}(R_2) - R_1 f_k(R_1) f_{k'}(R_1)] \right\},$$

$$F_{kk'l}^{rr} = \frac{1}{V} \int_{R_1}^{R_2} r^2 dr f_k(r) \frac{\partial}{\partial r} \int_{R_1}^{R_2} r'^2 dr' \tau_l'(r, r') f_{k'}(r'),$$

$$F_{kk'l}^{\theta r} = \frac{1}{V} \int_{R_1}^{R_2} r dr f_k(r) \int_{R_1}^{R_2} r'^2 dr' \tau_l'(r, r') f_{k'}(r') = F_{k'l}^{r\theta},$$

$$F_{kk'l}^{\theta\theta} = \frac{1}{V} \int_{R_1}^{R_2} r dr f_k(r) \int_{R_1}^{R_2} r' dr' \tau_l(r, r') f_{k'}(r'), \quad (31)$$

where

$$\tau_l(r, r') = \begin{cases} \frac{r^l}{r'^{l+1}}, & r < r' \\ \frac{r'^l}{r^{l+1}}, & r > r' \end{cases}, \quad \tau_l'(r, r') = \frac{\partial \tau_l(r, r')}{\partial r'}. \quad (32)$$

Deriving Eq. (25) (in the part concerning the magneto-static energy) we used the following relation

$$\frac{1}{|\mathbf{r} - \mathbf{r}'|} = 4\pi \sum_{l=0}^{\infty} \frac{\tau_l(r, r')}{2l+1} \sum_{m=-l}^l Y_l^m(\theta, \varphi) Y_l^{m*}(\theta', \varphi'). \quad (33)$$

Note that the presence of the factor $\ln(1/a_{ex})$ in the definition of $[a_{ex}^{(0)}]^2$, as well as the fact that we restrict integration over x in the formula (28) (despite the fact that the integral is convergent) is due to the presence of the vortex cores located at the poles of the particle. We neglect the effect of these cores. In Eq. (25), the terms proportional to $F_{kk'l}^{ab}$ come from the magnetostatic energy of the particle. They play the role of demagnetizing factors. Terms proportional to a_{ex}^2 or $(a_{ex}^{(m)})^2$ arise due to the exchange energy. For relatively small k and l , these terms are small compared to the “demagnetizing factors”, since in the case under consideration $a_{ex} \sim 10^{-2}$. This limit is different from that considered, e.g., in Refs. 14–16. At the same time, for large k or l , the contributions from the exchange energy become large (these are proportional to k^2 and l^2 , respectively). This ensures that Eq. (25) can be solved by restriction of the summation over k and l to some finite values, if we are interested in not too high frequencies.

Thus, we obtained a system of linear equations for the components of magnetization \tilde{m}^{aklm} , connecting them with the components of the external alternating magnetic field \tilde{h}^{aklm} . An important property of these equations is that they are diagonal in the azimuth index m . This is directly related to the geometry of the problem under

consideration. In arbitrarily directed, homogeneous external field¹⁷, only the components \tilde{h}^{aklm} with $m = 0$ and $m = \pm 1$ are nonzero. Accordingly, only the magnetization components \tilde{m}^{aklm} with the same indices m will be excited. We solve the system (25) numerically by truncating the summation over k and l to some values of $K_{\max} - 1$ and $L_{\max} - 1$, respectively. Let us introduce the vectors \tilde{m}_m and \tilde{h}_m , having dimension $2K_{\max}L_{\max}$, in the form

$$\tilde{m}_m = \begin{pmatrix} \tilde{m}_m^r \\ \tilde{m}_m^\theta \end{pmatrix} = \begin{pmatrix} \{\tilde{m}^{rklm}\} \\ \{\tilde{m}^{\theta klm}\} \end{pmatrix}, \quad (34)$$

$$\tilde{h}_m = \begin{pmatrix} \tilde{h}_m^r \\ \tilde{h}_m^\theta \end{pmatrix} = \begin{pmatrix} \{\tilde{h}^{rklm}\} \\ \{\tilde{h}^{\theta klm}\} \end{pmatrix}. \quad (35)$$

Then, in the frequency representation, Eq. (25) can be rewritten in the matrix form as

$$\left[-\frac{i\omega}{\omega_s} \begin{pmatrix} \alpha & -1 \\ 1 & \alpha \end{pmatrix} + \begin{pmatrix} \hat{\Lambda}_m^{rr} & (\hat{\Lambda}_m^{\theta r})^T \\ \hat{\Lambda}_m^{\theta r} & \hat{\Lambda}_m^{\theta\theta} \end{pmatrix} \right] \begin{pmatrix} \tilde{m}_m^r \\ \tilde{m}_m^\theta \end{pmatrix} = \begin{pmatrix} \tilde{h}_m^r \\ \tilde{h}_m^\theta \end{pmatrix}, \quad (36)$$

where elements of the matrices $\hat{\Lambda}_m^{ab}$ are obviously determined from Eq. (25). It is not difficult to verify that the matrices $\hat{\Lambda}_m^{ab}$ are real, and the matrices $\hat{\Lambda}_m^{aa}$ are symmetric. Let us denote the matrix in square brackets in Eq. (36) as $\hat{\chi}_m^{-1}(\omega)$. The inverse matrices with $m = 0, \pm 1$, the elements of which we denote as $\tilde{\chi}_{bk'l}^{aklm}(\omega)$, determine the susceptibility of the particle in the chosen representation. In the next Section, we will derive the corresponding expression for the susceptibility of a particle in the Cartesian coordinate system, as well as an expression for the magnetic permeability of the composite as a function of $\tilde{\chi}_{bk'l}^{aklm}(\omega)$.

III. PERMEABILITY OF THE COMPOSITE

In Cartesian coordinates and frequency representation, the relationship between the magnetization of a particle and an external field is defined as

$$m^\alpha(\mathbf{r}; \omega) = \frac{1}{V} \int_V d^3\mathbf{r}' \chi_\beta^\alpha(\mathbf{r}, \mathbf{r}'; \omega) h^\beta(\mathbf{r}'; \omega), \quad (37)$$

where $\chi_\beta^\alpha(\mathbf{r}, \mathbf{r}'; \omega)$ is the particle susceptibility tensor in Cartesian coordinate system. It is related to that in spherical coordinate system by the equality

$$\chi_\beta^\alpha(\mathbf{r}, \mathbf{r}'; \omega) = \frac{\partial x^\alpha}{\partial x^a} \chi_b^a(\mathbf{r}, \mathbf{r}'; \omega) \frac{\partial x'^b}{\partial x'^\beta}. \quad (38)$$

In a homogeneous field, the averaged magnetization of a particle is

$$m^\alpha(\omega) = \frac{1}{V^2} \int_V d^3\mathbf{r} \int_V d^3\mathbf{r}' \chi_\beta^\alpha(\mathbf{r}, \mathbf{r}'; \omega) h^\beta(\omega) \equiv \chi_\beta^\alpha(\omega) h^\beta(\omega). \quad (39)$$

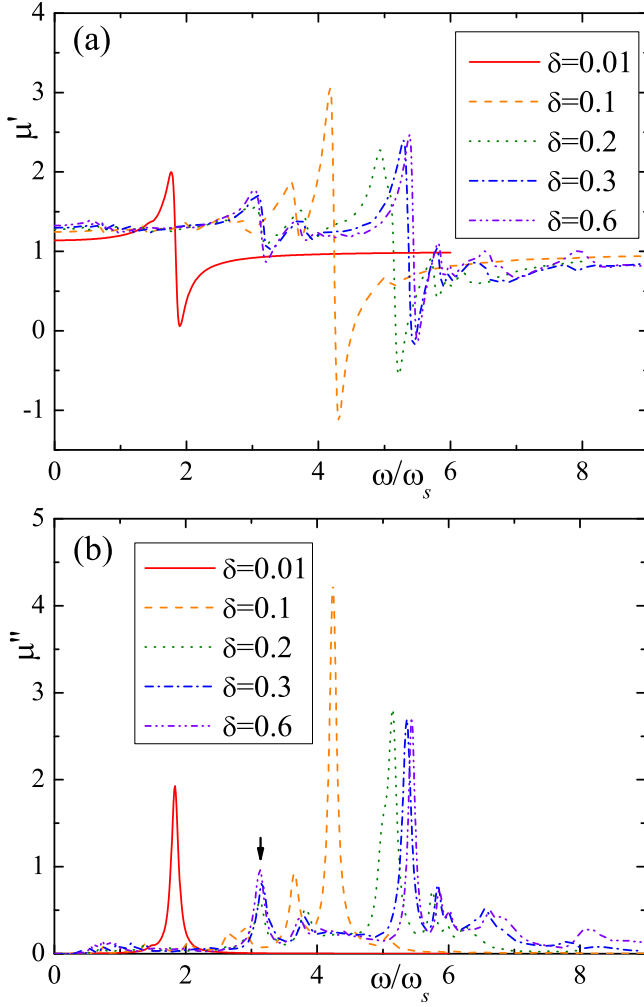


FIG. 2. Frequency dependencies of real (a) and imaginary (b) parts of the permeability of the composite, calculated for five values (see the legend) of the shell thickness d . Model parameters: $\beta = 0.1$, $a_{ex} = 0.01$, $p_c = 0.15$, $\alpha = 0.01$.

$$\mu(\omega) = 1 + \frac{4\pi p_F}{9} \sum_{m=-1}^1 \left[\tilde{\chi}_{r01m}^{r01m}(\omega) + \sum_{l=|m|}^{\infty} (\tilde{\chi}_{\theta 0lm}^{r01m}(\omega) + \tilde{\chi}_{r01m}^{\theta 0lm}(\omega)) D_{1l}^{(m)} + \sum_{l=|m|}^{\infty} \sum_{l'=|m|}^{\infty} \tilde{\chi}_{\theta 0l'm}^{\theta 0lm}(\omega) D_{1l}^{(m)} D_{1l'}^{(m)} \right], \quad (43)$$

where $D_{1l'}^{(m)}$ is given by Eq. (26). Deriving formula (43), we took into account that for the selected set of functions $f_k(r)$ we have (see Appendix) $f_0(r) = \sqrt{4\pi} = \text{const}$, and

$$\frac{1}{V} \int_{R_1}^{R_2} r^2 dr f_k(r) = 0, \quad k > 0, \quad (44)$$

due to the orthogonality of the radial functions.

For a given frequency ω we calculate $\tilde{\chi}_{bk'l'm}^{aklm}(\omega)$ and $\mu(\omega)$ numerically. For all the results below, wherever it is not specified in the text, we choose $K_{\max} = 36$ and

We assume that the directions of the local z axes of the particles are randomly distributed in the composite. Then, for the susceptibility of the composite, we obtain

$$\chi(\omega) = \frac{p_F}{3} \chi_{\alpha}^{\alpha}(\omega) = \frac{p_F}{3V^2} \int d^3\mathbf{r} \int d^3\mathbf{r}' \frac{\partial x^{\alpha}}{\partial x^{\alpha}} \chi_b^{\alpha}(\mathbf{r}, \mathbf{r}'; \omega) \frac{\partial x'^b}{\partial x'^{\alpha}}, \quad (40)$$

where p_F is the volume fraction of the ferromagnet. It is related to the volume fraction of particles in the composite, p_c , by the formula

$$p_F = p_c \left[1 - \left(\frac{1-\delta}{1+\delta} \right)^3 \right], \quad \delta = \frac{R_2 - R_1}{R_2 + R_1} = \frac{2d}{R_0}. \quad (41)$$

Note that the formula (40) was obtained by neglecting the interaction of particles with each other. As we have shown above, particles in the equilibrium configuration do not create a magnetic field (if vortex cores are ignored). Therefore, it can be expected that the approximation of non-interacting particles is adequate even for sufficiently large p_c . Particle susceptibility tensor in spherical coordinates, $\chi_b^{\alpha}(\mathbf{r}, \mathbf{r}'; \omega)$, is related to the matrices we obtained above $\tilde{\chi}_{bk'l'm}^{aklm}(\omega)$ through the equality

$$\chi_b^{\alpha}(\mathbf{r}, \mathbf{r}'; \omega) = \frac{1}{\mathcal{Z}^{\alpha}(r)} \left[\sum_{m=-1}^1 \sum_{kk'=0}^{\infty} \sum_{ll'=|m|}^{\infty} f_k(r) Y_l^m(\theta, \varphi) \times \tilde{\chi}_{bk'l'm}^{aklm}(\omega) f_{k'}(r') Y_{l'}^m(\theta', \varphi')^* \right] \mathcal{Z}^b(r'). \quad (42)$$

Substituting this expression into Eq. (40) and integrating over the coordinates, we obtain for the magnetic permeability of the composite, $\mu(\omega) = 1 + 4\pi\chi(\omega)$, the formula

$L_{\max} = 151$. Figure 2 shows the frequency dependencies of the permeability of the composite, calculated for several values of the shell thickness d . The imaginary part of the permeability is characterized by one main peak and several secondary peaks, which are located at both lower and higher frequencies. When parameter $\delta = 2d/R_0$ is small enough ($\delta \lesssim 0.3$) the main peak shifts to the right as δ increases. This correlates with the results obtained in Ref. 8. Such a behavior can be explained as following. For small δ one can consider only one, homogeneous, radial mode, taking $K_{\max} = 1$. The parameters F_{00l}^{ab} can

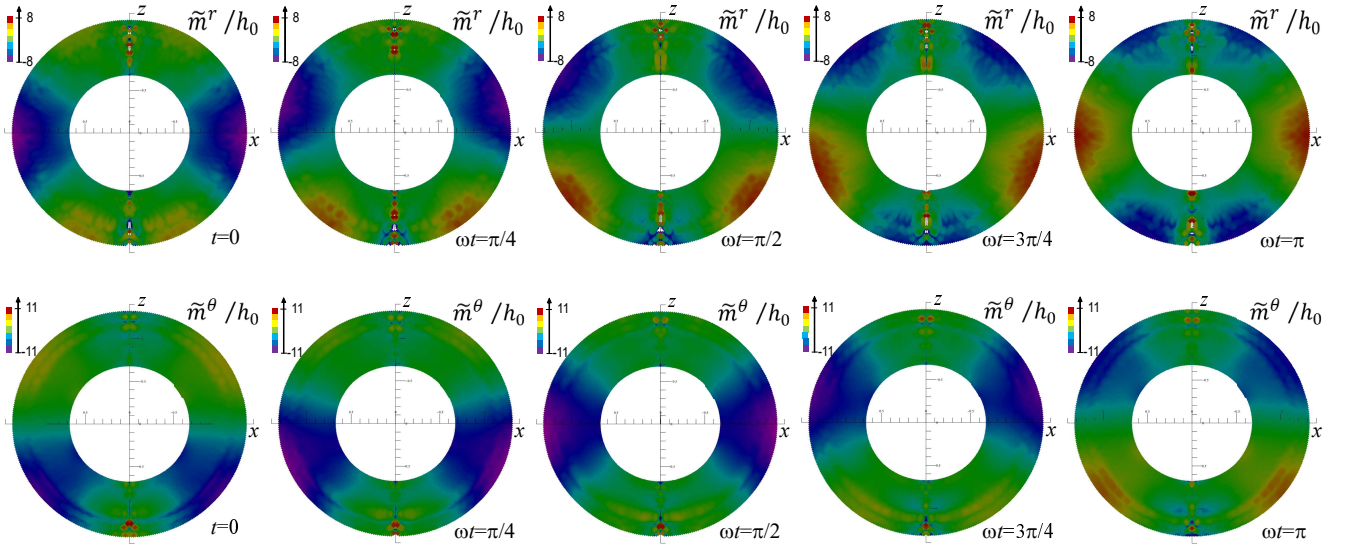


FIG. 3. The color plots of the radial (upper panels) and polar (lower panels) components of the particle's magnetization in the xz plane, calculated at different t in the range $0 \leq \omega t \leq \pi$. The oscillation frequency corresponds to the main resonance. External ac magnetic field is parallel to the z axis. Model parameters: $\delta = 0.3$, $\beta = 0.1$, $a_{ex} = 0.01$, $\alpha = 0.01$.

be calculated analytically. We will not present corresponding formulas here but will limit ourselves to the asymptotics at $\delta \rightarrow 0$ and $l \rightarrow \infty$. We have

$$\begin{aligned}
 F_{00l}^{rrr} &\rightarrow \begin{cases} 2l+1, & \delta \rightarrow 0 \\ 1/\delta, & l \rightarrow \infty \end{cases}, & F_{00l}^{r\theta} &\rightarrow \begin{cases} -\delta, & \delta \rightarrow 0 \\ -1/l, & l \rightarrow \infty \end{cases}, \\
 F_{00l}^{\theta\theta} &\rightarrow \begin{cases} 2\delta, & \delta \rightarrow 0 \\ 2/l, & l \rightarrow \infty \end{cases}. & & (45)
 \end{aligned}$$

Note that the asymptotics for $\delta \rightarrow 0$ are valid only when $l\delta \ll 1$. We see that the parameters F_{00l}^{rrr} and $F_{00l}^{\theta\theta}$ increase in magnitude when δ increases, which leads to a shift in the resonant frequency to the right. For larger $\delta (\gtrsim 0.3)$, the position of the main resonance practically does not change. Indeed, the main resonance frequency cannot go to infinity when $\delta \rightarrow 1$. When $\delta \lesssim 0.1$, the amplitude of the main resonance peak increases with δ . This is because the volume fraction of the ferromagnet, p_F , almost linearly increases with δ when δ is small. For larger δ , the p_F increases more slowly. Thus, the amplitude of the main resonance start to decrease when the position of the main peak shifts to higher frequencies. Let us estimate the characteristic values of the main resonance frequencies for the curves shown in Fig. 2. Taking $M_s = 1700$ Gs (as for Fe), we will have $\omega_s/2\pi \cong 4.75$ GHz. Thus, the resonance frequencies lay approximately in the range 8–25 GHz. These resonance frequencies are bit higher than that observed experimentally in Refs. 4–6.

Let us analyze the character of the magnetization oscillations at different frequencies. We consider first the situation when the magnetic field is directed along the z axis of a particle, i.e. perpendicular to $\mathbf{M}_0(\mathbf{r})$ (outside the vortex core). Using the expression (37), as well as the formula (42) for the susceptibility of the particle, we obtain the formula for the particle's magnetization in the field $\mathbf{h} = \mathbf{e}_z h_0 e^{-i\omega t}$ in the form

$$\begin{aligned}
 \tilde{m}^a(\mathbf{r}, t) = \text{Re} \left\{ \sum_{k=0}^{\infty} \sum_{l=0}^{\infty} f_k(r) \sqrt{\frac{2l+1}{12\pi}} P_l(\cos\theta) \times \right. & (46) \\
 \left. \left[\tilde{\chi}_{r010}^{akl0}(\omega) + \sum_{l'=0}^{\infty} \tilde{\chi}_{\theta 0l'0}^{akl0}(\omega) D_{1l'}^{(0)} \right] e^{-i\omega t} \right\} h_0.
 \end{aligned}$$

We see, that the magnetization does not depend on the angle φ . For the chosen direction of the magnetic field the magnetization oscillations are determined by the susceptibility matrix $\tilde{\chi}_{bk'l'm}^{aklm}(\omega)$ with $m = 0$. Figure 3 shows the snapshots of the $\tilde{m}^a(\mathbf{r}, t)$ in the xz plane taken at five different t in the range $0 \leq \omega t \leq \pi$. The frequency ω corresponds to the main resonance (the highest peak in Fig. 2). The distribution of $\tilde{m}^a(\mathbf{r}, t)$ is spatially non-uniform. Neglecting the sharp peaks at the poles, the largest magnitude of oscillations exists at the equator of the particle. The spatial profiles of the magnetization components $\tilde{m}^r(\theta, t)$ and $\tilde{m}^\theta(\theta, t)$ are phase shifted by $\pi/2$ relative to each other, which corresponds to the rotation of the local magnetization around an axis lying in the xy plane and tangent to the surface of the particle.

Let us consider now the case when the magnetic field

is parallel to the x axis. In this case the particle's mag-

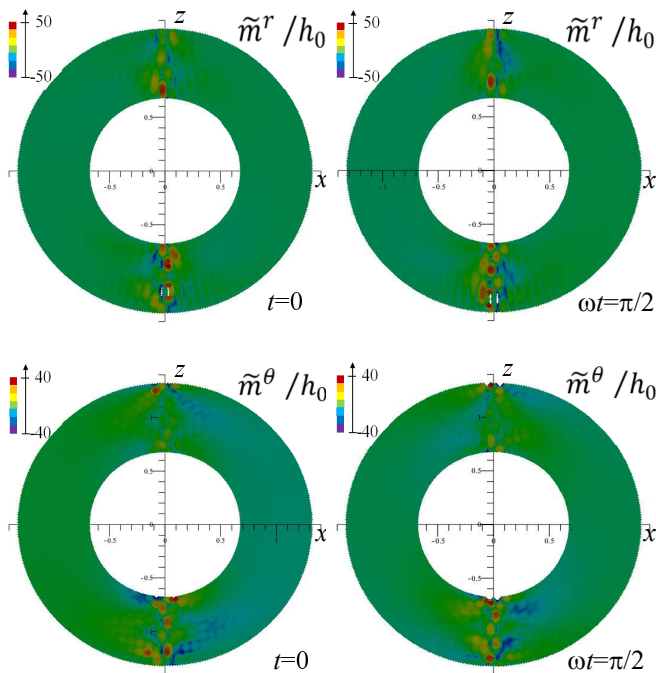


FIG. 4. The color plots of the radial (upper panels) and polar (lower panels) components of the particle's magnetization in the xz plane, calculated at different t in the range $0 \leq \omega t \leq \pi$. The oscillation frequency corresponds to resonance marked by the arrow in Fig. 2(b). External ac magnetic field is parallel to the x axis. Model parameters: $\delta = 0.3$, $\beta = 0.1$, $a_{ex} = 0.01$, $\alpha = 0.01$.

netization is given by the formula

$$\tilde{m}^a(\mathbf{r}, t) = -\text{Re} \left\{ \sum_{k=0}^{\infty} \sum_{l=1}^{\infty} f_k(r) \sqrt{\frac{2l+1}{6\pi l(l+1)}} P_l^1(\cos \theta) \times \left[\tilde{\chi}_{r011}^{akl1}(\omega) + \sum_{l'=1}^{\infty} \tilde{\chi}_{\theta 0l'1}^{akl1}(\omega) D_{l'l}^{(1)} \right] e^{-i\omega t} \right\} \cos \varphi h_0. \quad (47)$$

We see that the magnetization is controlled now by the susceptibility matrix $\tilde{\chi}_{bk'l'm}^{aklm}(\omega)$ with $m = 1$. The magnetization is proportional to $\cos \varphi$, that is, the largest amplitude of oscillations exists in the xz plane. Our calculations show that at the main resonance frequency, the magnetic moments of the particle are excited only near the vortex core, and the amplitude of these oscillations is smaller than that for the case of the magnetic field parallel to the z axis. Thus, the main contribution to the imaginary part of the permeability of the composite at the main resonance frequency comes from the particles with local z axes parallel to the applied ac field.

Besides main resonance peak, the imaginary part of the permeability of the composite shows also several smaller peaks, laying both below and above main resonance. We study the magnetization distribution at different pronounced secondary resonances and found similar behavior of the magnetization for all considered frequencies. We show the results corresponding to the frequency

marked by the arrow in Fig. 2(b). Our calculations show that for all secondary resonances studied the largest amplitude of oscillations exists when the magnetic field is *perpendicular* to the z axis of the particle. Figure 4 shows the distribution of $\tilde{m}^a(\mathbf{r}, t)$ in the xz plane ($\cos \varphi = \pm 1$) calculated at $\omega t = 0$ and $\omega t = \pi/2$ (magnetic field is parallel to the x axis). We see that the magnetization is excited only near the vortex core. The amplitude of these oscillations is several times larger than that at the main resonance. Thus, the main contribution to secondary resonances shown in Fig. 2 comes from the particles with local z axes perpendicular to the ac magnetic field.

IV. PERMEABILITY OF THE COMPOSITE IN THE LIMIT $d/R_0 \rightarrow 0$ AND $l_{ex}/R_0 \rightarrow 0$

In this section, we will derive an analytical formula for the permeability of the composite in the limit of $d/R_0 \rightarrow 0$ and $a_{ex} = l_{ex}/R_0 \rightarrow 0$. For the thin shell, one can consider only first, homogeneous, radial mode, ignoring other modes. In the limit $a_{ex} \rightarrow 0$, we can also neglect the contributions to the Landau-Lifshitz equation (25) from the energy of the exchange interaction. Next, according to the formula (45), we have $F_{00l}^{r\theta} \rightarrow 0$, $F_{00l}^{\theta\theta} \rightarrow 0$, and $F_{00l}^{rr} \rightarrow 2l+1$ when $\delta \rightarrow 0$. Ignoring the contributions from $F_{00l}^{r\theta}$ and $F_{00l}^{\theta\theta}$, we obtain that the equations (25) become diagonal on the index l . Such equations can be solved analytically. Substituting the found expressions for $\tilde{\chi}_{b0lm}^{a0lm}$ into the formula (43), we obtain the expression for the magnetic permeability of the composite in the form

$$\mu(\omega) = 1 + \frac{p_F}{3} (4\pi\omega_s)^2 \times \frac{[A(1 + \beta/4\pi) + \beta/4\pi] - i\alpha\omega(1+A)/(4\pi\omega_s)}{\omega_r^2 - (1 + \alpha^2)\omega^2 - 2i\alpha\omega\omega_s(2\pi + \beta)}, \quad (48)$$

where

$$\omega_r = \omega_s \sqrt{\beta(4\pi + \beta)} \quad (49)$$

is the resonance frequency, and

$$A = \frac{1}{3} \left(\sum_{l=0}^{\infty} D_{1l}^{(0)} \right)^2 + \frac{2}{3} \left(\sum_{l=0}^{\infty} D_{1l}^{(1)} \right)^2. \quad (50)$$

Performing numerical summation in the formula (50), we obtain $A \cong 1.76$. Note that in the considered limit, the resonance frequency of the composite (49) coincides with the resonance frequency of the thin film with uniaxial magnetic anisotropy. In addition, the expression (48) for the permeability is similar to that for the thin film (after averaging over the direction of the magnetic field), with the only difference that for the thin film $A \equiv 1$.

Figure 5 shows the dependence of the main resonance frequency on the anisotropy parameter β , calculated numerically using Eq. (25) for two different shell thicknesses δ (in these calculations we take $K_{\max} = 10$). The curve

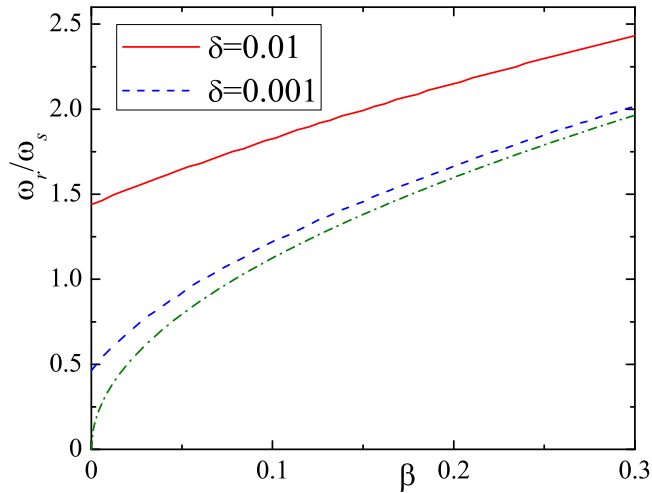


FIG. 5. The dependence of the main resonance frequency on the anisotropy parameter β , calculated for the shell thickness $\delta = 0.01$ (red solid curve) and $\delta = 0.001$ (blue dashed curve). Green dot-dashed curve corresponds to Eq. (49). Model parameters: $a_{ex} = 0.01$, $\alpha = 0.01$.

$\omega_r(\beta)$ with ω_r from Eq. (49) is also shown in this figure for comparison. We see, that Eq. (49) underestimate the resonance frequency. For very thin shell ($\delta = 0.001$) formula (49) is adequate approximation for the resonance frequency when the anisotropy parameter is not very close to zero. However, already for $\delta = 0.01$, disagreement between analytical expression (49) and the numerical result is quite strong. This can be explained by the fact that for such δ we cannot neglect the “demagnetizing factors” $4\pi F_{00l}^{\theta\theta} \cong 8\pi\delta$ and $4\pi F_{00l}^{rr\theta} \cong -4\pi\delta$ in Eq. (25) in comparison to β .

V. STABILITY OF THE STATIC MAGNETIC CONFIGURATION. SELF-OSCILLATIONS OF THE MAGNETIZATION

In this section we study the self-oscillations of the magnetization and show that the vortex magnetic configuration shown in Fig. 1 more likely corresponds to the local minimum of energy. In order to obtain the equations for self-oscillations, it is necessary to take in Eq. (36) $\alpha = 0$ and $\tilde{h}_m^a = 0$. As a result, Eq. (36) can be rewritten as

$$\omega^2 \begin{pmatrix} \tilde{m}_m^r \\ \tilde{m}_m^\theta \end{pmatrix} + \hat{\Omega}_m^2 \begin{pmatrix} \tilde{m}_m^r \\ \tilde{m}_m^\theta \end{pmatrix} = 0, \quad (51)$$

where

$$\hat{\Omega}_m^2 = \begin{pmatrix} \hat{\Lambda}_m^{\theta\theta} \hat{\Lambda}_m^{rr} - \left(\hat{\Lambda}_m^{\theta r} \right)^2 & \hat{\Lambda}_m^{\theta\theta} \left(\hat{\Lambda}_m^{\theta r} \right)^T - \hat{\Lambda}_m^{\theta r} \hat{\Lambda}_m^{\theta\theta} \\ \hat{\Lambda}_m^{rr} \hat{\Lambda}_m^{\theta r} - \left(\hat{\Lambda}_m^{\theta r} \right)^T \hat{\Lambda}_m^{rr} & \hat{\Lambda}_m^{rr} \hat{\Lambda}_m^{\theta\theta} - \left[\left(\hat{\Lambda}_m^{\theta r} \right)^T \right]^2 \end{pmatrix}. \quad (52)$$

This equation is the eigenvalue equation for the matrix $\hat{\Omega}_m^2$. We are only interested in matrices with $m = 0$ and

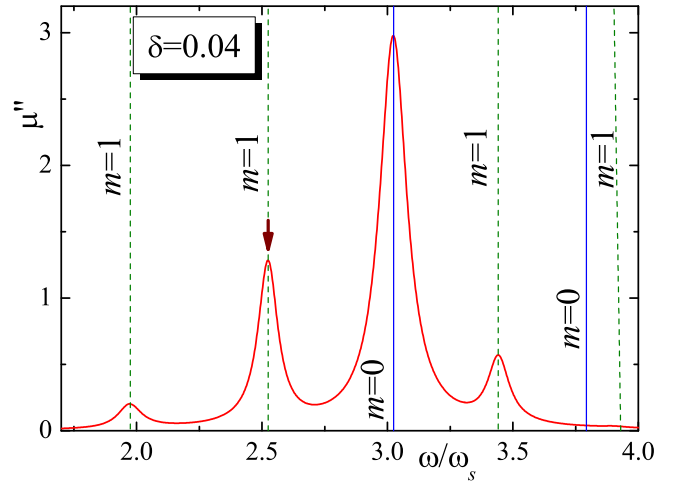


FIG. 6. The frequency dependence of the imaginary part of the permeability, calculated at $\delta = 0.04$. Other parameters of the model are: $\beta = 0.1$, $a_{ex} = 0.01$, $p_c = 0.15$, $\alpha = 0.01$. Vertical lines mark the square roots of the eigenfrequencies of the matrices $\hat{\Omega}_0^2$ (solid lines) and $\hat{\Omega}_1^2$ (dashed lines).

$m = \pm 1$, since only oscillations with such m are excited in the homogeneous magnetic field. It can also be shown that the matrices with $m = +1$ and $m = -1$ are identical. Therefore, we only examine the matrices $\hat{\Omega}_0^2$ and $\hat{\Omega}_1^2$. The analysis shows that for all values of the model parameters considered in this paper, the eigenvalues of these matrices, ω_{mS}^2 ($S = 1, 2, \dots, 2K_{\max}L_{\max}$), turn out to be real and positive. It indicates¹⁸ that the equilibrium magnetic configuration considered here indeed corresponds to the local minimum of energy. In addition, it turns out that all eigenvalues of the matrices $\hat{\Omega}_m^2$ are doubly degenerate.

For large K_{\max} and L_{\max} the set of eigenfrequencies ω_{mS} is quite dense. For this reason, to be more illustrative, we consider here the thin shell taking into account only one, homogeneous, radial mode. Figure 6 shows the frequency dependence of the imaginary part of the composite’s permeability, calculated at $\delta = 0.04$ in the frequency range $1.7 < \omega/\omega_s < 4$. The vertical lines in this figure show all ω_{0S} and ω_{1S} laying within this frequency range. We see that the main resonance corresponds to some eigenfrequency ω_{0S} , while all side resonances correspond to the eigenfrequencies ω_{1S} . Note also that there are some eigenfrequencies that do not correspond to any peaks in the imaginary part of the permeability. This can be explained by the presence of a selection rule prohibiting the excitation of certain self-oscillations in a homogeneous field. These selection rules are apparently controlled by the parameters $D_{1l}^{(m)}$ [see formula (43)], for which the equality $D_{1l}^{(m)} = 0$ is valid for $\text{mod}(l, 2) = 1$ due to the symmetry of spherical harmonics.

Let us now consider the spatial profiles of the self-oscillations of the magnetization corresponding to some resonant frequencies. If \tilde{m}_S^{aklm} is some eigenfunction of the matrix $\hat{\Omega}_m^2$, then the magnetization fluctuations, cor-

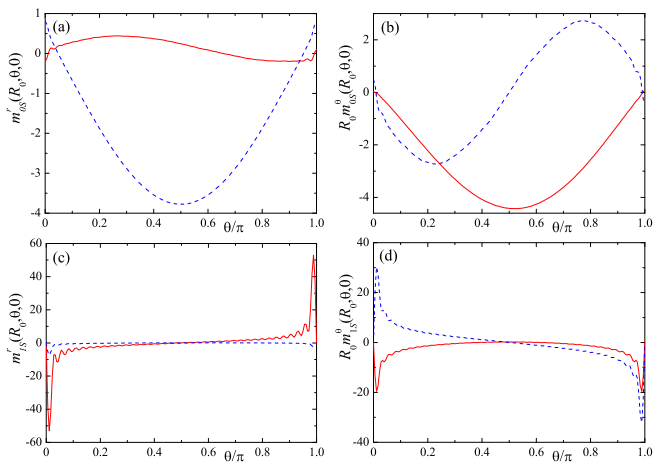


FIG. 7. The dependencies of the radial (a, c) and polar (b, d) components of the self magnetization oscillations on the polar angle θ corresponding to the main resonance (panels a and b) and the resonance indicated by the arrow in Fig. 6 (panels c and d). Model parameters: $\delta = 0.04$, $\beta = 0.1$, $a_{ex} = 0.01$.

responding to this mode, are calculated by the formula

$$\tilde{m}_{S_m}^a(\mathbf{r}) = \sum_{k=0}^{\infty} \sum_{l=|m|}^{\infty} \tilde{m}_S^{aklm} f_k(r) Y_l^m(\theta, \varphi). \quad (53)$$

When only one, homogeneous, radial mode is taken into account, the functions $\tilde{m}_{S_m}^a(\mathbf{r})$ do not depend on r . Further, for $m = 0$ these functions do also not depend on φ , while for $m = \pm 1$ this dependence reduces to $e^{\pm i\varphi}$. Since all eigenfrequencies turn out to be doubly degenerate, each eigenfrequency will correspond to two eigenfunctions \tilde{m}_S^{aklm} . Calculations show that all eigenfunctions of \tilde{m}_S^{aklm} are real-valued. Figures 7(a,b) show the dependencies $\tilde{m}_{S_0}^a(\mathbf{r})$ and $\tilde{m}_{S_0}^b(\mathbf{r})$ on the polar angle θ for the eigenfunctions of the matrix $\hat{\Omega}_0^2$ corresponding to the main resonance frequency. We see that the oscillations at the poles are practically not excited. In this case, the profiles $\tilde{m}_{S_0}^a(\mathbf{r})$ are in many ways similar to those for the magnetization fluctuations in the ac field parallel to the z axis of the particle at times $\omega t = 0$ and $\omega t = \pi/2$ (see Fig. 3). We observe a completely different picture for the self oscillations corresponding to the matrix $\hat{\Omega}_1^2$. Figures 7(c, d) show the dependencies of $\tilde{m}_{S_1}^a(R_0, \theta, 0)$ on the angle θ for the eigenfunctions corresponding to the resonance frequency indicated by the arrow in the Fig. 6. We see that fluctuations occur mainly near the poles of the particle. This correlates with the results shown in Fig. 4.

VI. DISCUSSION

Thus, we studied the response of the composite consisting of hollow spherical ferromagnetic particles to an alternating magnetic field. We analyzed the behavior

of the magnetic permeability as a function of the ratio $\delta = 2d/R_0$. We showed that the main resonance frequency shifts to the right as δ increases. This behavior seems natural and finds its analogy with the behavior of resonance frequency in a thin film. Indeed, for a film with longitudinal dimensions L and thickness d , the components of the demagnetization tensor along the film, $N_{x,y}$, increase with the increase of the ratio d/L : $N_{x,y} \propto d/L \ln(L/d)$. In our case, the role of demagnetizing factors $N_{x,y}$ is played by the parameters F_{00l}^{θ} and $F_{00l}^{\theta\theta}$, which increase linearly with δ at small δ . This leads to a shift of the resonant frequency to the right. In the limit of $\delta \rightarrow 0$ we obtained an analytical expression for the permeability of the composite, and showed that it is in many ways similar to that for a thin film.

The main assumption of this work is the vortex structure of the equilibrium magnetization configuration, schematically shown in Fig. 1. This structure is characterized by the presence of two vortex cores located at the poles of the particle, the influence of which we neglect. At the same time, we have shown that the side resonances of the permeability of the composite correspond to the magnetization oscillations near the poles. Therefore, the question of whether these side resonances are an artifact of the approximation under consideration or whether they are really characteristic of the equilibrium magnetic configuration under consideration requires separate consideration. In particular, it is possible to perform a micromagnetic calculation of the equilibrium configuration and then solve the Landau-Lifshitz equations linearized around the found magnetization distribution.

Another significant assumption of this work is a special type of uniaxial magnetic anisotropy: the axis of anisotropy is not fixed, but rotates in space along with the magnetization. Strictly speaking, this leads to the fact that the magnetic configuration under consideration corresponds to a certain extreme of energy (a local minimum, as shown in Section V). If we assume that the particle has a certain fixed axis of anisotropy, this will generally lead to a change in its ground state magnetic configuration, which can significantly complicate calculations. Indeed, in this case we can expect more complicated dependence of the magnetization on the azimuthal angle φ . At the same time, in the case of weak magnetic anisotropy, $\beta \ll 1$, these effects can be assumed to be insignificant.

In this paper we completely neglected the skin effect. This can be done if the thickness d of the shell is much smaller than the skin depth l_s . Let us evaluate here the characteristic thicknesses d for which this can be done. The skin depth can be estimated using the formula⁷

$$l_s = \frac{c}{\sqrt{2\pi\sigma\omega\mu_{st}}},$$

where c is the speed of light, while σ and μ_{st} are the conductivity and static permeability of the particle, respectively. Let us estimate l_s at the frequency corresponding to the main resonance for the composite with $\delta = 0.2$,

$\omega \cong 5\omega_s$ (see Fig. 2). Assuming $M_s = 1700$ Gs and $\sigma = 9 \times 10^{16} \text{ sec}^{-1}$ (as for Fe), we obtain $l_s \approx 1/\sqrt{\mu_{st}} \mu\text{m}$. The static permeability of the particle can be estimated from the results obtained above using the formula $\mu_{st} = 1 + (\mu(0) - 1)/p_F$, where $\mu(0)$ is the permeability of the composite at zero frequency. Thus, for $\delta = 0.2$, we obtain $\mu_{st} \approx 3.8$, and $l_s \approx 0.5 \mu\text{m}$. For particles' diameters $D \sim 1 \mu\text{m}$ and $d \lesssim R_2$ we have $d \lesssim l_s$. Thus, we are at the edge of the applicability of the absence skin effect approximation. How the skin effect affects the results obtained will be considered in future studies.

Appendix A: Construction of radial orthogonal functions

In this Appendix, we describe an algorithm for construction of the radial functions orthogonal with weight r^2 and satisfying the boundary conditions (23). To do this, we will first represent them as

$$f_k(r) = \sqrt{\frac{V}{d}} \frac{g_k(x(r))}{r}, \quad x(r) = \frac{r - R_1}{d}, \quad 0 \leq x \leq 1. \quad (\text{A1})$$

The functions $g_k(x)$ should be orthogonal with weight 1,

$$\int_0^1 dx g_k(x) g_{k'}(x) = \delta_{kk'}, \quad (\text{A2})$$

and satisfy the boundary conditions

$$\begin{cases} g'_k(0) - \frac{2\delta}{1-\delta} g_k(0) = 0 \\ g'_k(1) - \frac{2\delta}{1+\delta} g_k(1) = 0 \end{cases}, \quad (\text{A3})$$

following from the conditions (23). The functions $g_k(x)$ can be constructed in different ways. Here we choose the following. Consider trigonometric functions of the form

$$y_k(x) = A_k \sin(\mu_k x) + B_k \cos(\mu_k x). \quad (\text{A4})$$

We will require them to satisfy the boundary conditions (A3). Then we obtain,

$$y_k(x) = C_k \left[\frac{2\delta}{(1-\delta)\mu_k} \sin(\mu_k x) + \cos(\mu_k x) \right], \quad (\text{A5})$$

where the coefficients C_k are found from the normalization condition, and μ_k should satisfy the equation

$$\left(\mu_k + \frac{4\delta^2}{(1-\delta^2)\mu_k} \right) \tan \mu_k = \frac{4\delta^2}{1-\delta^2}. \quad (\text{A6})$$

Note that if μ_k is the root of Eq. (A6), then $-\mu_k$ will be the root of the same equation with the same function $y_k(x)$. Therefore, we can consider only the non-negative roots of Eq. (A6). There is infinite number of non-negative roots of Eq. (A6), which we will arrange in ascending order of the index k : $\mu_0 < \mu_1 < \dots$

Further, we cannot identify the functions $y_k(x)$ with the desired functions $g_k(x)$, because the functions $y_k(x)$ are not orthogonal. We will use the following orthogonalization procedure. We take $g_0(x) = y_0(x)$, while all other $g_k(x)$ are constructed by using the following recurrent formula

$$g_k(x) = b_k \left[y_k(x) - \sum_{j=0}^{k-1} \left(\int_0^1 dx' g_j(x') y_k(x') \times g_j(x) \right) \right], \quad (\text{A7})$$

where the coefficients b_k are found from the normalization condition. It is easy to see that the functions $g_k(x)$ constructed in this way are orthonormal.

Finally, we observe that the smallest non-negative root of Eq. (A6) is $\mu_0 = 0$. The corresponding function $g_0(x) = y_0(x)$ is obtained by taking the limit $\mu_0 \rightarrow 0$ in the formula (A5). As a result, we obtain

$$y_0(x) = C_0 \left[\frac{2x\delta}{1-\delta} + 1 \right]. \quad (\text{A8})$$

It is easy to verify from this equation and equation (A1) that $f_0(r) = \text{const}$, or, taking into account the normalization condition, $f_0(r) = \sqrt{4\pi}$.

¹ Z. Li and Z. Yang, "Microwave absorption properties and mechanism for hollow Fe₃O₄ nanosphere composites," *Journal of Magnetism and Magnetic Materials* **387**, 131 (2015).
² I. Shanenkov, A. Sivkov, A. Ivashutenko, V. Zhuravlev, Q. Guo, L. Li, G. Li, G. Wei, and W. Han, "Magnetite hollow microspheres with a broad absorption bandwidth of 11.9 GHz: toward promising lightweight electromagnetic microwave absorption," *Phys. Chem. Chem. Phys.* **19**, 19975 (2017).
³ M. Sui, X. Sun, H. Lou, X. Li, X. Lv, L. Li, and G. Gu, "Synthesis of hollow Fe₃O₄ particles via one-step solvothermal approach for microwave absorption materials: effect of

reactant concentration, reaction temperature and reaction time," *Journal of Materials Science: Materials in Electronics* **29**, 7539 (2018).

⁴ A. Kosevich, E. Petrushevich, S. Maklakov, A. Naboko, E. Kolesnikov, D. Petrov, P. Zezyulina, K. Pokholok, D. Filimonov, and M. Han, "Low Weight Hollow Microspheres of Iron with Thin Dielectric Coating: Synthesis and Microwave Permeability," *Coatings* **10** (2020).

⁵ A. V. Artemova, S. S. Maklakov, A. V. Osipov, D. A. Petrov, A. O. Shiryayev, K. N. Rozanov, and A. N. Lagarkov, "The Size Dependence of Microwave Permeability of Hollow Iron Particles," *Sensors* **22** (2022).

⁶ A. V. Artemova, S. S. Maklakov, A. O. Shiryayev, A. V.

- Osipov, D. A. Petrov, K. N. Rozanov, and A. N. Lagarkov, "Influence of Hydrogen Reduction Stage Conditions on the Microwave Properties of Fine Iron Powders Obtained via a Spray-Pyrolysis Technique," *Magnetism* **3**, 90 (2023).
- ⁷ L. D. Landau and E. M. Lifshits, *Electrodynamics of continuous media* (Pergamon Press Oxford, 1946).
- ⁸ C. McKeever, F. Y. Ogrin, and M. M. Aziz, "Microwave magnetization dynamics in ferromagnetic spherical nanoshells," *Phys. Rev. B* **100**, 054425 (2019).
- ⁹ V. P. Kravchuk, D. D. Sheka, R. Streubel, D. Makarov, O. G. Schmidt, and Y. Gaididei, "Out-of-surface vortices in spherical shells," *Physical Review B* **85**, 144433 (2012).
- ¹⁰ A. Sboychakov, "About magnetic energy of ferromagnetic particle with cavity," *Modern Electrodynamics* **5(7)**, 15 (2023).
- ¹¹ N. Hirano, S. Kobayashi, E. Nomura, M. Chiba, H. Kasai, Z. Akase, T. Akashi, A. Sugawara, and H. Shinada, "Magnetic vortex structure for hollow Fe_3O_4 spherical sub-micron particles," *Applied Physics Letters* **119**, 132401 (2021).
- ¹² L. D. Landau, *The classical theory of fields*, vol. 2 (Elsevier, 2013).
- ¹³ J. Brown, William Fuller, "Micromagnetics, Domains, and Resonance," *Journal of Applied Physics* **30**, S62 (1959), https://pubs.aip.org/aip/jap/article-pdf/30/4/S62/18320709/s62_1_online.pdf.
- ¹⁴ A. Aharoni, "Exchange resonance modes in a ferromagnetic sphere," *Journal of Applied Physics* **69**, 7762 (1991), https://pubs.aip.org/aip/jap/article-pdf/69/11/7762/18643195/7762_1_online.pdf.
- ¹⁵ A. Aharoni, "Effect of surface anisotropy on the exchange resonance modes," *Journal of applied physics* **81**, 830 (1997).
- ¹⁶ G. Viau, F. Fiévet-Vincent, F. Fiévet, P. Toneguzzo, F. Ravel, and O. Acher, "Size dependence of microwave permeability of spherical ferromagnetic particles," *Journal of applied physics* **81**, 2749 (1997).
- ¹⁷ At frequencies of the order of 1–10 GHz, the wavelength of the incident radiation is much larger than the particle's size. So, the magnetic field can be considered homogeneous.
- ¹⁸ To prove that the vortex magnetic configuration corresponds to the energy minimum we should analyse matrices Ω_m^2 for all m .